

Spin-Orbit Coupling Fluctuations as a Mechanism of Spin Decoherence

M. Martens,^{1,2,*} J. van Tol,² N.S. Dalal,^{2,3} S. Bertaina,⁴ and I. Chiorescu^{1,2,†}

¹*Department of Physics, Florida State University, Tallahassee, Florida 32306, USA*

²*The National High Magnetic Field Laboratory, Tallahassee, Florida 32310, USA*

³*Department of Chemistry & Biochemistry, Florida State University, Tallahassee, Florida 32306, USA*

⁴*Aix-Marseille Université, CNRS, IM2NP UMR7334, 13397 cedex 20, Marseille, France.*

(Dated: May 14, 2015)

Mechanisms of spin decoherence are of significance in developing solid state qubits. We performed a systematic study on spin decoherence in the compound $\text{K}_6[\text{V}_{15}\text{As}_6\text{O}_{42}(\text{D}_2\text{O})] \cdot 8\text{D}_2\text{O}$, using high-field Electron Spin Resonance (ESR). By analyzing the anisotropy of resonance linewidths as a function of orientation, temperature and field, we study fluctuations in the spin Hamiltonian, and find the spin-orbit term as major decoherence source. The demonstrated mechanism can alter the lifetime of any spin qubit and we discuss how to mitigate it by sample design and field orientation.

PACS numbers: 75.50.Xx, 71.70.Ej, 76.30.-v, 03.67.-a

In solid-state systems, interactions between electronic spins and their environment are the limiting factor of spin phase lifetime, or decoherence time. Important advances have been recently realized in demonstrating long-lived spin coherence via spin dilution [1–6] and isolating a spin in non-magnetic cages [7], for instance. Phonons are an important source of energy relaxation and thus spin-lattice interactions need to be reduced, usually by cooling to sufficiently low temperatures. The presence of a lattice can be felt by spins through orbital symmetries and spin-orbit coupling. An isolated free electron has a spin angular momentum associated with a g -factor $g_e = 2.00232$. In many molecular compounds containing 3d elements, the orbital angular momentum is quenched and one expects a g -factor only slightly different from g_e due to the admixture of excited orbital states [8] into the ground state caused by spin-orbit coupling. In this Letter, we present observational evidence that fluctuations in the spin-orbit interaction can be a significant source of spin decoherence. This is accomplished by analyzing shape and orientation anisotropy of ESR linewidths at 120, 241, and 336 GHz, of the molecular compound $\text{K}_6[\text{V}_{15}^{\text{IV}}\text{As}_6^{\text{III}}\text{O}_{42}(\text{D}_2\text{O})] \cdot 8\text{D}_2\text{O}$, V_{15} in short. This system has been shown to have high coherence at low temperatures [9], has demonstrated coherent spin oscillations [5] and interesting out of equilibrium spin dynamics due to phonon bottlenecking [10, 11]. However the details of the spin decoherence are still not fully understood. This study points to a new decoherence mechanism, fluctuation in the spin-orbit term, and how to optimize the decoherence in spin qubits.

The V_{15} cluster anions form a lattice with trigonal symmetry ($a = 14.029 \text{ \AA}$, $\alpha = 79.26^\circ$, $V = 2632 \text{ \AA}^3$) containing two clusters per unit cell. Individual molecules have fifteen $\text{V}^{\text{IV}} s = 1/2$ ions arranged into three layers, two non-planar hexagons sandwiching a triangle (see Fig. 1(a)). Exchange couplings between the spins in the triangle and hexagons exceed 100 K [12, 13] and at low temperatures this spin system can be modeled as a tri-

angle of spins $1/2$. The Hamiltonian for this three spin model is given by [14]:

$$\mathcal{H}_{st} = \mathcal{H}_Z + \mathcal{H}_J + \mathcal{H}_{DM} \quad (1)$$

where \mathcal{H}_Z represents the Zeeman splitting, \mathcal{H}_J is the symmetric exchange term, and \mathcal{H}_{DM} is the anti-symmetric Dzyaloshinsky-Moriya (DM) term (see [14] for a detailed formulation). \mathcal{H}_{st} eigenvalues are shown in Fig. 1(b) and are used to calculate resonant field positions B_{res} of the ESR spectra through the method of first moments [14]. Additionally, dipolar interactions between molecular spins in the crystal are described by:

$$\mathcal{H}_{dz} = \frac{3\mu_0}{8\pi} \mu_B^2 \sum_q g_p(\theta) g_q(\theta) S_p S_q \frac{(1 - 3 \cos^2 \phi_{pq})}{d_{pq}^3} \quad (2)$$

with μ_0 the vacuum permeability, μ_B the Bohr magneton, θ the angle between the applied field \vec{B}_0 and the z axis (z is \perp to triangle plane and is also the symmetry c axis of the molecule), d_{pq} the distance between sites p and q , $g_{p,q}(\theta) = (g_a^2 \sin^2 \theta + g_c^2 \cos^2 \theta)^{1/2}$, $g_{c,a}$ the g -tensor components parallel and perpendicular to the z axis, $\vec{S}_{p,q}$ the molecular spin, ϕ_{pq} the angle between \vec{S}_p and \vec{d}_{pq} . Components of this dipolar Hamiltonian are most responsible for fluctuations in the system, as detailed below.

The linewidth of ESR signals can be significantly affected by exchange interactions. In V_{15} the intramolecular couplings are large and the exchange narrowing effect [15] collapses the $(2I + 1)^{15}$ resonances ($I = 7/2$ for ^{51}V) into one and it also acts to average out fluctuations related to \mathcal{H}_{st} . This leaves fluctuations in \mathcal{H}_{dz} as being the major contributor to spin decoherence.

There are three possible sources of fluctuation in Eq.(2), the first being the geometrical factor $(1 - 3 \cos^2 \phi_{pq}) d_{pq}^{-3} = R_{pq}(t)$ since both d_{pq} and ϕ_{pq} can fluctuate (here, t represents time). This case is described by Bloembergen *et al.* [16] (Nuclear Magnetic Resonance case) and Kubo and Tomita [15] (ESR case). If $R_{pq}(t)$

fluctuates randomly, its correlation function decays exponentially $\langle R(t)R(0) \rangle = R^2 + r^2 \exp(-t/\tau_{dip})$ with a Fourier spectrum:

$$J_R(\nu) = r^2 \frac{2\tau_{dip}}{1 + 4\pi^2\nu^2\tau_{dip}^2} \quad (3)$$

where R is an average value of the geometric term $\sum_{p \neq q} R_{pq}$, r is an average size of $R(t)$'s fluctuations and the correlation time τ_{dip} is a characteristic of the random motion. This procedure is described generally by Ather-ton [17] and can be applied to any stationary random function that is independent of the time origin. The inverse square of the decoherence time T_2 is proportional to $\int J_R(\nu)d\nu$ [15, 16]. Therefore, the decoherence rate depends directly on r .

Another fluctuation source comes from thermal excitations to different S_z states of $S_{p,q}$ and their effect on the second moment of a resonance line has been theoretically analyzed in detail [18–20]. Following Kambe and Usui [19], the fluctuations Fourier spectrum is directly proportional to a temperature dependent factor:

$$KU(T) = \langle S_z^2 \rangle_T - \langle S_z \rangle_T^2 = S^2 \frac{d}{dy} B_s(y) \quad (4)$$

where $B_s(y)$ is the Brillouin function, $y = T_z S/T$, $T_z = \hbar F_{mw}/k_B$ (F_{mw} is the microwave excitation frequency), and $S = 3/2$ is the total spin state of the three-spin triangle. $KU(T)$ is thus similar to r^2 in Eq. (3) and originates from a $S_z^2(t)$ correlation function similar to $\langle R(t)R(0) \rangle$. This formulation breaks down for temperatures near or below the ordering temperature of the spin system. For V_{15} this temperature is ~ 0.01 K [21] which is well below the temperatures used in this study.

Fluctuations of $g(\theta)$ in Eq. (2) can also reduce the decoherence time. Deviation of the g -factor away from g_e is due to the spin-orbit interaction [8]:

$$\mathbf{g} = g_e \mathbf{I} - 2\lambda \mathbf{\Lambda} \quad (5)$$

where \mathbf{g} is the g -tensor (diagonal $[g_a, g_a, g_c]$ for V_{15}), \mathbf{I} is the unit matrix, λ is the spin-orbit coupling constant and $\mathbf{\Lambda}$ is a tensor defined in terms of the matrix elements of the orbital angular momentum \mathbf{L} . In general terms, $\mathbf{\Lambda}$ is the coupling between the ground and excited orbitals divided by their energy separation. Here, we focus on relative fluctuations in the coupling term with an average size ξ (assumed isotropic) which induce fluctuations in the g -factor and \mathcal{H}_{dz} . An average fluctuation in the g -factor can thus be written as:

$$\delta g(\theta) = \xi (g(\theta) - g_e). \quad (6)$$

Assuming $g(\theta)$ is a stationary function with small random fluctuations, the temperature dependent correlation function of a fluctuating $\mathcal{H}_{dz}(t)$ is:

$$\begin{aligned} G_{dz}(t) &= \langle \mathcal{H}_{dz}(t) \mathcal{H}_{dz}(0) \rangle \\ &= \beta \langle g(t)g(0) \rangle^2 KU(T) \langle R(t)R(0) \rangle \end{aligned} \quad (7)$$

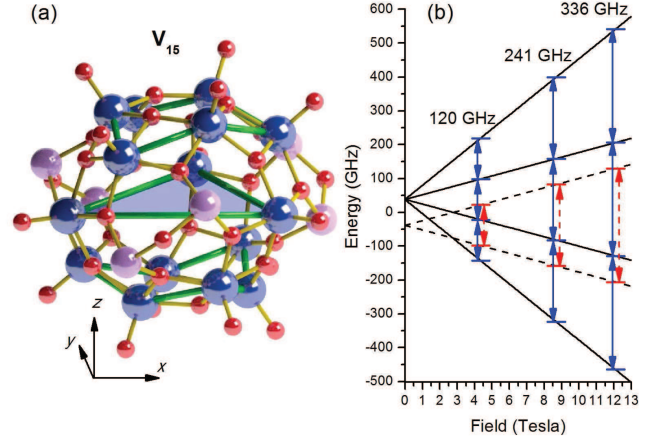


FIG. 1. (Color online) (a) Ball-and-stick representation of V_{15} , with the $s = 1/2$ V ions in blue. The x axis is along one side of the triangle while the z axis is perpendicular to the triangle plane and represents the c axis of the crystal unit cell. (b) Level diagram of the three spin model with positions of the three experimental frequencies shown. Dashed lines show the $S = 1/2$ doublets with the red dashed arrows indicating those transitions. Lines show the $S = 3/2$ quartet with blue arrows indicating the transitions; the resonance fields are averaged in the first moment calculation of B_{res} at a given frequency.

where $\langle g(t)g(0) \rangle = g(\theta)^2 + (\delta g(\theta))^2 \exp(-t/\tau_g)$, τ_g is the correlation time of g -factor fluctuations, and $\beta = \left(\frac{3\mu_0\mu_B}{8\pi}\right)^2$. As in Eq. (3), this leads to a spectral intensity:

$$\begin{aligned} J_{dz}(\nu) &= \sqrt{\frac{2}{\pi}} \beta KU(T) \left\{ g(\theta)^4 r^2 \frac{\tau_{dip}}{1 + 4\pi^2\tau_{dip}^2\nu^2} \right. \\ &\quad + 2g^2(\theta)\delta g^2(\theta) \left[R^2 \frac{\tau_g}{1 + 4\pi^2\tau_g^2\nu^2} + r^2 \frac{\tau_{gd}}{1 + 4\pi^2\tau_{gd}^2\nu^2} \right] \\ &\quad \left. + \delta g^4(\theta) \left[R^2 \frac{\tau_g/2}{1 + \pi^2\tau_g^2\nu^2} + r^2 \frac{\tau'_{gd}}{1 + 4\pi^2\tau_{gd}^2\nu^2} \right] \right\} \end{aligned} \quad (8)$$

where $\tau_{gd}^{-1} = \tau_g^{-1} + \tau_{dip}^{-1}$ and $\tau'_{gd} = 2\tau_g^{-1} + \tau_{dip}^{-1}$. In absence of g -factor fluctuations, Eq. (8) reduces to the first term in the sum as in [19] [see the geometrical term in Eq. (3)]. Such a temperature dependence of the linewidth has been experimentally demonstrated in Fe_8 [22–24], nitrogen-vacancy color centers in diamond [25] and other studies seem to confirm it as well [26, 27]. If the g -value does fluctuate then all three terms in Eq. (8) represent sources of decoherence. Because T_2^2 is inversely proportional to $\int J_{dz}(\nu)d\nu$, an important consequence is that one can combine different decoherence sources by summing their effect on $J_{dz}(\nu)$ as follows:

$$\frac{1}{T_2^2} \approx \sum_i \frac{1}{T_{2i}^2}, \quad (9)$$

similar to the well-known fact that the sum of uncorrelated variances is equal to the total variance. Addi-

tionally, the weight of each term in the sum depends on, or can be tuned with, the field angle θ . Here we show that for V_{15} , fluctuations in the g -value and thus, in the spin-orbit interaction, are affecting the coherence time.

Continuous-wave ESR measurements at 120, 241, and 336 GHz are performed using the quasioptical superheterodyne spectrometer at the National High Magnetic Field Laboratory [28, 29], with a sweepable 12.5 T superconducting magnet (homogeneity of 10^{-5} over 1 cm^3). Sample temperature can be varied from room temperature down to 2.5 K. A single crystal of volume $\lesssim 0.1 \text{ mm}^3$ was positioned on a rotating stage allowing for continuous change of the angle θ between \vec{B}_0 and the c axis of the molecule following the procedure described in our previous work [14]. The homogeneity of the magnet compared to the size of the crystal allows us to ignore \vec{B}_0 as a source of broadening. The applied fields are above 4 T, past the crossing of the $S = 1/2$ doublet and $S = 3/2$ quartet, such that the ground state of the system is in the $S = 3/2$ quartet (see Fig. 1(b)).

ESR spectra at temperatures $T = 4\text{--}60 \text{ K}$ for $\vec{B}_0 \parallel$ and \perp to c -axis ($\theta = 0^\circ, 90^\circ$ respectively) show a Lorentzian (homogenous) lineshape. Representative spectra with Lorentzian and Gaussian fits are shown in Fig. 2(a) for comparison. The temperature dependence of the linewidth is shown in Fig. 2(c) for three microwave frequencies F_{mw} . Compared to measurements made at lower fields [30], where the ground state is in the $S = 1/2$ doublet, the linewidths are ~ 10 times narrower. Plotted is the full width at half maximum (FWHM) of the Lorentzian fits vs T/F_{mw} to underline that the temperature dependent mechanism of decoherence in the system qualitatively follows the temperature behavior predicted by $KU(T)$ [Eq. (4)]. Additionally, there is no hyperfine structure visible in the spectra (exchange narrowing) since the 3d electrons of V interact with the nuclei of several other V ions due to the large exchange couplings ($\sim 10^2 \text{ K}$) within the molecule. Due to these properties of the measured line width and shape, we can estimate T_2 to be the inverse of the FWHM.

There are two distinct curves in Fig. 2(c), dependent on the orientation of \vec{B}_0 . To probe this orientation dependence, the linewidth is measured as a function of the field angle θ [see Fig. 2(b)]. The narrowest linewidth occurs when $\theta = 0^\circ$ ($\vec{B}_0 \parallel c$ axis) while the largest occurs at $\theta = 90^\circ$ (\vec{B}_0 in the triangle plane). This implies more decoherence the further $g(\theta)$ gets from g_e since $g(0^\circ) = g_c \approx 1.98$ and $g(90^\circ) = g_a \approx 1.95$. This means that the FWHM and the first term in Eq. 8 have angular dependences that are 180° out of phase. This property of the V_{15} compound makes it particularly suitable to study the effect of spin-orbit fluctuations. Furthermore, the fact that the width is largest when $g(\theta)$ is minimum and vice-versa rules out exchange narrowing being the cause of this anisotropy since it would require a linewidth

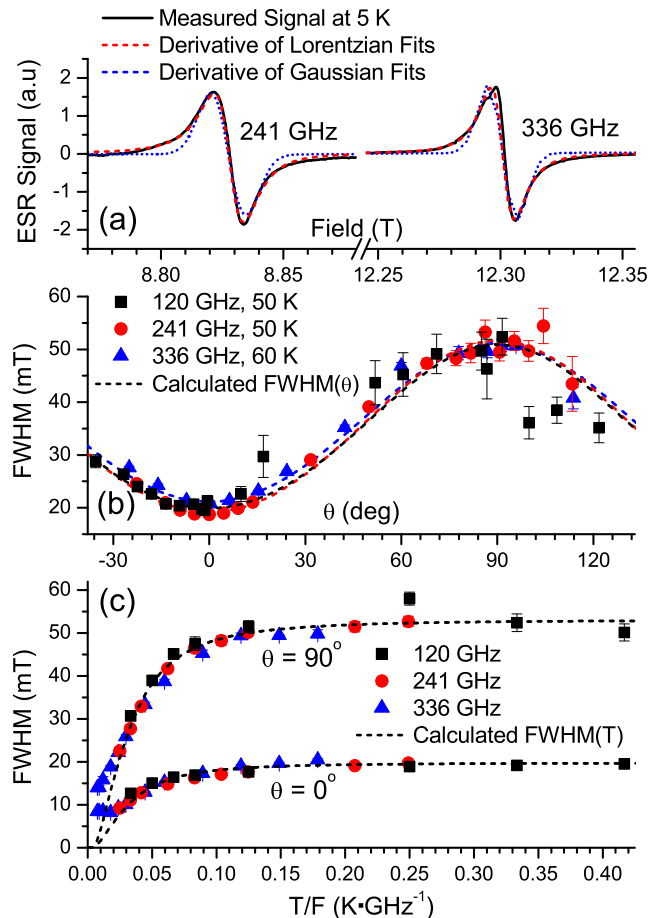


FIG. 2. (Color online) (a) Typical measurements of the derivative of the absorption χ'' at 336 GHz and 241 GHz with derivative of Gaussian (blue dotted line) and Lorentzian fits (red dashed line). (b) FWHM of Lorentzian fits as a function of field angle θ measured at three frequencies: 336 GHz (blue triangles), 241 GHz (red circles) and 120 GHz (black squares). The dashed lines are calculated widths as a function of θ using Eq. (11). (c) FWHM of Lorentzian fits vs temperature/frequency for the 3 studied frequencies. Dashed lines are calculated FWHM(T) for $\theta = 0^\circ$ and 90° .

$\propto (1 + \cos^2 \theta)$ [15], as in the case of CsCuCl_3 [31]. Consequently, this out-of-phase behavior provides strong evidence that $\delta g(\theta) \neq 0$ and terms in Eq. (8) containing it must be considered.

The measured field linewidths can be converted into broadening of the molecule eigenvalues through exact diagonalization of the three-spin Hamiltonian, Eq. (1). We calculate the minimum and maximum excitation frequencies $F_{min,max}$ leading to resonance fields $B_{max,min}$ using the first moment method [14]. Their difference is:

$$\Delta E = h(F_{max} - F_{min}). \quad (10)$$

As mentioned above, since $1/T_2 \propto \sqrt{\int J_{dz}(\nu)}$ [15, 16] the linewidth square is proportional to the prefactor $KU(T)$ and either R or r depending on which term in the sum

of integrals from Eq. (8) dominates. This leads to the following fit equation [see also Eq. (6)]:

$$\Delta E^2 = KU(T) \left[A^2 (g(\theta) - g_e)^4 + a^2 g^2(\theta) (g(\theta) - g_e)^2 \right] \quad (11)$$

where A and a are fit parameters describing the out-of-phase behavior discussed above. Taking $\Delta E(0^\circ)$ and $\Delta E(90^\circ)$ we solve for A and a and calculate the curve $\Delta E(\theta)$ using these values. This curve is then converted back to units of Tesla by solving the static Hamiltonian. We calculate the resonance fields for two frequencies $F'_{min,max} = F_{mw} \pm \Delta E(\theta)/2h$ and take their difference as the calculated value of the FWHM of an experimental signal. Shown in Fig. 2(b) are the field angle dependencies of the FWHM for the three frequencies used in this study as well as calculated widths using Eq. (11).

Parameters A and a are then averaged, giving values $\bar{A} = 320 \pm 34$ GHz and $\bar{a} = 10.8 \pm 1.6$ GHz, and are further used to test the validity of model (11). The values of ΔE (converted to Tesla) vs T/F_{mw} are fitted with Eq. (11) for two angles $\theta = 0^\circ$ and 90° corresponding to g -factors $g_c = 1.981$ and $g_a = 1.953$ respectively. The fit using \bar{A} and \bar{a} is in very good agreement with the experimental data, as shown with dotted line in Fig. 2(c). On the low end of the ratio T/F_{mw} one observes a saturation of the linewidth, attributed to other decoherence sources.

Our study provides insight on how to analyze combined sources of decoherence and, in particular, how to mitigate the effects of spin-orbit fluctuations. It is evident from Eqs. (6) and (7) that the g -tensor should be as close as possible to g_e . In molecular compounds this can be achieved by engineering the ligands type since local symmetry affects the diagonal values of the g -tensor of a magnetic ion. Aside from material design by chemical methods, $J_{dz}(\nu)$ can be minimized by applying the magnetic field at a specific angle θ . For V_{15} , this would be $\theta = 0$ for which the decoherence times reaches several nanoseconds. This time can reach ~ 400 ns by reducing r in $J_{dz}(\nu)$ via dilution in liquid state, thus allowing the observation of Rabi oscillations and spin-echoes [5].

In conclusion, we find that the angular dependence of the ESR linewidth of V_{15} cannot be explained through solely a spin flip-flop model [19], nor through exchange narrowing theory [15]. This dependence is out-of-phase with the g -factor orientation anisotropy and we introduce a quantitative model based on random fluctuations of g . This type of fluctuation can be detrimental to any spin-based qubit implementation in solid-state systems and we discuss mitigation methods based on chemical engineering and experimental parameters.

We wish to acknowledge David Zipse and Vasanth Ramachandran for their help in growing V_{15} crystals. This work was supported by NSF Grant No. DMR-1206267 and CNRS-PICS CoDyLow. The NHMFL is supported by Cooperative Agreement Grant No. DMR-1157490 and the state of Florida.

* martens@magnet.fsu.edu

† ic@magnet.fsu.edu

- [1] S. Bertaina, L. Chen, N. Groll, J. Van Tol, N. S. Dalal, and I. Chiorescu, Phys. Rev. Lett. **102**, 050501 (2009).
- [2] S. Nellutla, K.-Y. Choi, M. Pati, J. van Tol, I. Chiorescu, and N. S. Dalal, Phys. Rev. Lett. **99**, 137601 (2007).
- [3] S. Bertaina, S. Gambarelli, A. Tkachuk, I. N. Kurkin, B. Malkin, A. Stepanov, and B. Barbara, Nature Nanotechnology, **39**.
- [4] M. V. G. Dutt, L. Childress, L. Jiang, E. Togan, J. Maze, F. Jelezko, A. S. Zibrov, P. R. Hemmer, and M. D. Lukin, Science **316**, 1312 (2007).
- [5] S. Bertaina, S. Gambarelli, T. Mitra, B. Tsukerblat, A. Müller, and B. Barbara, Nature **453**, 203 (2008).
- [6] A. Ardavan, O. Rival, J. J. L. Morton, S. J. Blundell, A. M. Tyryshkin, G. A. Timco, and R. E. P. Winpenny, Phys. Rev. Lett. **98**, 057201 (2007).
- [7] G. W. Morley, J. van Tol, A. Ardavan, K. Porfyrakis, J. Zhang, and G. A. D. Briggs, Phys. Rev. Lett. **98**, 220501 (2007).
- [8] M. H. L. Pryce, Proceedings of the Physical Society. A. **63**, 25 (1950).
- [9] V. V. Dobrovitski, M. I. Katsnelson, and B. N. Harmon, Phys. Rev. Lett. **84**, 3458 (2000).
- [10] I. Chiorescu, W. Wernsdorfer, A. Müller, H. Bögge, and B. Barbara, Journal of Magnetism and Magnetic Materials **221**, 103 (2000).
- [11] I. Chiorescu, W. Wernsdorfer, A. Müller, H. Bögge, and B. Barbara, Physical Review Letters **84**, 3454 (2000).
- [12] D. Gatteschi, L. Pardi, A. L. Barra, A. Müller, and J. Döring, Nature **354**, 463 (1991).
- [13] A. L. Barra, D. Gatteschi, and L. Pardi, Journal of the American Chemical Society **114**, 8509 (1992).
- [14] M. Martens, J. van Tol, N. S. Dalal, S. Bertaina, B. Barbara, B. Tsukerblat, A. Müller, S. Garai, S. Miyashita, and I. Chiorescu, Physical Review B **89**, 195439 (2014).
- [15] R. Kubo and K. Tomita, Journal of the Physical Society of Japan **9**, 888 (1954).
- [16] N. Bloembergen, E. M. Purcell, and R. V. Pound, Phys. Rev. **73**, 679 (1948).
- [17] N. M. Atherton, *Electron Spin Resonance: theory and applications* (John Wiley & Sons, Inc., 1973).
- [18] M. H. L. Pryce and K. W. H. Stevens, Proceedings of the Physical Society. A. **63**, 36 (1950).
- [19] K. Kambe and T. Usui, Progress of Theoretical Physics **8**, 302 (1952).
- [20] M. McMillan and W. Opechowski, Canadian Journal of Physics **38**, 1168 (1960).
- [21] B. Barbara, I. Chiorescu, W. Wernsdorfer, H. Bögge, and A. Müller, Progress of Theoretical Physics Supplement, **357** (2002).
- [22] K. Park, M. A. Novotny, N. S. Dalal, S. Hill, and P. A. Rikvold, Physical Review B **66**, 144409 (2002).
- [23] S. Hill, S. Maccagnano, K. Park, R. M. Achey, J. M. North, and N. S. Dalal, Phys. Rev. B **65**, 224410 (2002).
- [24] S. Takahashi, J. van Tol, C. C. Beedle, D. N. Hendrickson, L.-C. Brunel, and M. S. Sherwin, Phys. Rev. Lett. **102**, 087603 (2009).
- [25] S. Takahashi, R. Hanson, J. van Tol, M. S. Sherwin, and D. D. Awschalom, Phys. Rev. Lett. **101**, 047601 (2008).
- [26] M. J. Graham, J. M. Zadrozny, M. Shiddiq, J. S. Anderson, M. S. Fataftah, S. Hill, and D. E. Freedman,

- Journal of the American Chemical Society **136**, 7623 (2014).
- [27] S. Takahashi, I. S. Tupitsyn, J. van Tol, C. C. Beedle, D. N. Hendrickson, and P. C. E. Stamp, Nature **476**, 76 (2011).
- [28] G. W. Morley, L.-C. Brunel, and J. van Tol, The Review of scientific instruments **79**, 064703 (2008).
- [29] J. van Tol, L.-C. Brunel, and R. J. Wylde, Review of Scientific Instruments **76**, 074101 (2005).
- [30] T. Sakon, K. Koyama, M. Motokawa, Y. Ajiro, A. Müller, and B. Barbara, Physica B: Condensed Matter **346-347**, 206 (2004).
- [31] H. Tanaka, K. Iio, and K. Nagata, Journal of the Physical Society of Japan **50**, 727 (1981).